




Adequacy of binary fluid and turbulator based natural circulation loop in parabolic trough collector

D. Chandan*, U. C. Arunachala**, K. Varun*

* Renewable Energy Center, Dept. of Mech. & Ind. Engg., Manipal Institute of Technology, Manipal Academy of Higher Education, Manipal – 576104, Karnataka State, India

** Renewable Energy Center, Dept. of Mech. & Ind. Engg., Manipal Institute of Technology, Manipal Academy of Higher Education, Manipal – 576104, Karnataka State, India

(chandand8005@gmail.com, arun.chandavar@manipal.edu, varun.naik.1995@gmail.com)

‡ Corresponding Author; U. C. Arunachala, Renewable Energy Center, Dept. of Mech. & Ind. Engg., Manipal Institute of Technology, Manipal Academy of Higher Education, Manipal – 576104, Karnataka State, India, Tel: +91-820-2925461, arun.chandavar@manipal.edu

Received: 02.10.2022 Accepted: 20.11.2022

Abstract- The natural circulation loop (NCL) is in the limelight due to its sustainable and reliable mechanism. It finds application mainly in nuclear and solar thermal power plants. However, the low flow rate of fluid within the loop and instability causes a hindrance to their widespread applications. Hence many instability restraining and heat transfer augmentation techniques have been studied, including the recent innovations viz. binary fluid and turbulators. In the present experimental study, a horizontal heater horizontal cooler loop is constructed, and its behaviour is compared with the Vijayan correlation. Later, the wire coil (pitch ratio = 4) effect is studied for the heat input range of 200 W to 600 W, which resulted in the heat transport efficiency improvement of 20% to 22% in the laminar region and 5% to 8% in other regimes with decreased mass flow rate as penalty. Even binary fluid (40% acetone + 60% water) influence is monitored separately for the same heat input range. The loop was neutrally stable for 200 W to 500 W heat input, and at 600 W, pulsation of loop fluid flow with high magnitude was noticed. Though binary fluid enhanced the mass flow rate, the heat transfer rate was not improved due to acetone's low specific heat value.

Keywords - Natural circulation loop; heat transfer augmentation; binary fluid; parabolic trough collector; turbulator in NCL.

1. Introduction

The motion that results from the continuous replacement of hot fluid in the vicinity of a hot body by a cold fluid is called a natural convection current. Natural circulation (NC) denotes the ability of a fluid in a system to circulate continuously, with a driving force created by gravity and changes in temperature. This driving force is known as 'buoyancy head' or 'driving head'. A natural circulation loop (NCL) consists of a heat source and heat sink connected by vertical legs, as shown in Fig. 1. In the heat source region, the fluid receives heat, thus becoming less dense, and it rises towards the cooler. Then it exchanges the heat with the sink, and relatively high-density fluid reaches back to the heater by gravity force. Thus, the fluid is said to flow due to natural convection, thereby avoiding external sources for pumping. Because of the passive nature of NCL, it finds several engineering applications, viz.

Automobile industry, Solar thermal energy conversion, electronics cooling, nuclear power plant etc.

Based on the orientation of the heater and cooler, NCL can be classified as horizontal heater horizontal cooler (HHHC), vertical heater horizontal cooler (VHHC), horizontal heater vertical cooler (HHVC), and vertical heater and vertical cooler (VHVC) configuration. Further, HHHC exhibits the highest loop fluid flow rate among the four versions due to the maximum centreline elevation. However, such single-phase NCL (SPNCL) has lower heat transportation capability and is susceptible to instability. But, considering the operating condition, SPNCL technology is still sustained, and research is focused on loop stability and heat transfer augmentation. Instability in NCL is more prominent due to the nonlinearity of the natural circulation process. Many techniques are in practice to curb instability

(particularly in HHHC configuration) and enhance heat transfer.

On the other hand, Solar energy is considered one of the prominent solutions for the present-day energy crisis [1], [2]. Solar energy can be extracted through: the photovoltaic route [3]–[5] and/or thermal route. The thermal route involves the use of solar concentrators to produce thermal power. Amongst different concentrators, parabolic troughs are prevalent due to simplicity in construction and operation. As a prominent application of NCL, HHHC design is thought of for parabolic trough collector (PTC) (Fig. 2). This logic makes sense as PTC demands noticeable pumping power for the heat transfer fluid (HTF) circulation. Here, the condenser (cooler) serves as the steam generator, while the evaporator (heater) is the recipient of concentrated radiation.

The loop diameter is the crucial factor during the construction of a loop. An experimental and theoretical study by Vijayan et al. [6] showed that instability occurs mainly in larger diameter loops due to the instability threshold decrement. Heater and cooler positions play an essential role in stability, as Vijayan et al. [7] found that VHVC configuration is more stable than HHHC. In an experimental study by Naveen et al. [8], it was found that the initial fluid level in the expansion tank affects the loop behaviour. Although the loop stabilised during start-up, during the power cut-off, it could not. Saha et al. [9] conducted a detailed experimental study and found that liquid inertia is important during the initial transition of the loop and as heat input increases, periodic to chaotic transformation takes in the loop. To curtail the instability in a large diameter (70 mm) HHHC loop (linked to PTC), Nakul and Arunachala [10] have performed 3-D computational analysis considering both loop tilt and orifice separately and combinedly. However, the latter version had better results for the defined configuration. An experimental investigation by Elton et al. [13] revealed the dependence of the operating procedure on the stability threshold of a rectangular loop. Even the influence of the orifice on the stability threshold was studied. A recent review by Elton and Arunachala [14] has thoroughly discussed loop stability and heat transfer augmentation methods, including nanofluids and air injection. But other methods, like binary fluid and turbulators, can also influence the NCL performance.

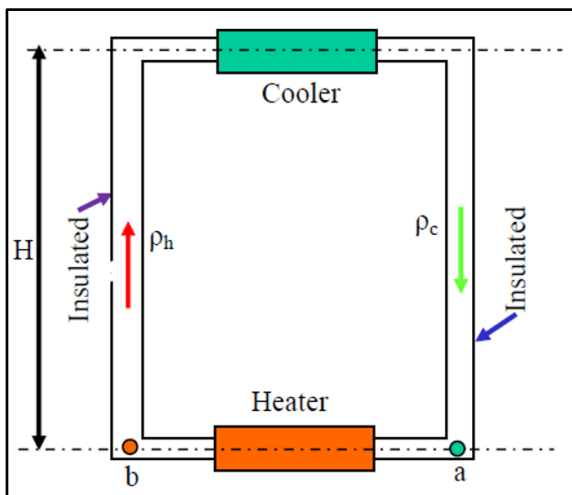


Fig. 1. Simple natural circulation loop [11]

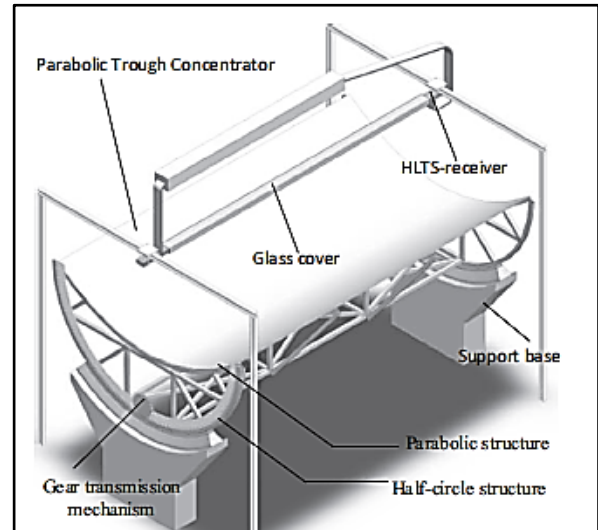


Fig. 2. NCL for PTC [12]

Pachgare and Mahalle [15] have conducted preliminary experiments on closed loop pulsating heat pipe (CLPHP) by employing different working fluids, viz. methanol, ethanol, acetone, water, and binary mixtures (1:1 mixture). With a filling ratio of 50% and heat inputs of 10-100 W, it was observed that at lower heat inputs, the binary mixtures outperformed the pure fluids (lower thermal resistance), whereas, at higher heat inputs, the trend was reversed. This is due to the dry-out phenomena (due to mixture boiling), which occurs at 80 W, 85 W, and 90 W for water-acetone, water-methanol, and water-ethanol respectively. Further, Pachgare and Mahalle [16] tested a CLPHP of the same dimensions but with two turns which also had a glass section for flow visualisation. The working fluids, filling ratio, and heat inputs were the same as in the previous study. Even a numerical CFD analysis was undertaken to analyse the flow phenomena. It was found that the water-acetone binary mixture yields the best results in terms of thermal resistance. Further, all the binary mixtures outperformed the pure fluids due to fewer turns in CLPHP, which restricts the dry-out phenomena. Cui et al. [17] tested the effect of binary fluid mixture ratios on the thermal resistance characteristics of CLPHP. The experiments were conducted with different methanol based binary fluid mixtures, i.e. methanol-water, methanol-acetone, and methanol-ethanol. The binary fluids were subjected to heater powers of 10-100 W, and the filling ratios employed were 45%, 62%, 70%, and 90%. It was observed that at a low filling ratio, methanol-water prevented dry-out at higher powers, and the thermal resistance of methanol-ethanol was in between that of pure methanol and ethanol. On the other hand, the thermal resistance of methanol-acetone was slightly lesser than pure methanol and acetone. At higher filling ratios, the thermal resistance of methanol-water was more than that of pure methanol and water. Thereby, it was deduced that the thermo-physical properties of binary fluid mixtures play a crucial role in CLPHP performance. However, such studies are limited to only heat pipe.

Kumar et al. [18] conducted an extensive review of conventional twisted type, alternate axis twisted tape with perforations and cuts, helical screw tape, wire coil inserts, and multiple twisted tape inserts application in steam boilers and

double pipe heat exchangers. It has been found that V-cut twisted tape transfers higher heat transfer than plain tube due to additional turbulence created by vorticity at the V-cuts. Wire coil-tape inserts enhance the heat transfer rate with minimal pressure drop, suitable for oil cooling devices, preheaters, and fire tube boilers. Awais and Bhuiyan [19] reviewed the use of Delta winglet and rectangular winglet type vortex generators and their effect on heat transfer rate and pressure loss on compact heat exchangers. The heat transfer improvement was observed behind the wake region and in the downstream region. The size, location, and attack angle of vortex generators are crucial to increase the heat transfer rate, but the location of vortex generators doesn't affect the pressure drop. The staggered arrangement of winglets is better than inline, and delta winglet pairs result in a higher heat transfer rate than rectangular winglet pairs.

Maradiya et al. [20] performed extensive experiments on inserts and the effect of their geometry on heat transfer rate. The twisted tape enhances the heat transfer rate in the laminar region but is not so effective in the turbulent region. However, wire coil is more effective in the turbulent region. Hence, a combination of twisted and wire coil inserts was suggested for better heat transfer in the tube heat exchangers. A review by Liu and Sakr [21], Sheikholeslami et al. [22], and Mousa et al. [23] also confirmed that inserts like twisted tape, wire coil, vortex generators, and conical tube had been extensively used in heat exchangers, preheaters, fire tube boilers, and air heating. Hence, from the reviews, the most popular inserts are twisted tape and wire coil inserts.

Keklikcioglu and Ozceyhan [24] have studied the effects of using convergent, convergent-divergent and divergent conical wire coils on the heat transfer in an ethylene glycol and water mixture. The use of conical wire coils enhances both the heat transfer rate and fluid friction, whereas adding ethylene glycol to water decreases the heat transfer rate with a rise in friction factor. The highest Nusselt number is obtained for the divergent conical wire coil in the case of 40:60 mixture, while the highest performance evaluation criteria is achieved for the divergent wire coil with water only. Owing to the potential application of sCO₂ Brayton cycle in nuclear engineering, Cong et al. [25] have numerically analysed the flow and heat transfer characteristics of sCO₂ in the straight channel (under supercritical pressure) with and without twisted tape. Twisted tape forms a swirling flow field with periodic spiral characteristics, which can effectively flatten the wall temperature distribution and narrow the range of temperature peak. Further, it can cut down drastic changes in temperature and suppress the deterioration of heat transfer during the flow, but the effect on the strong heat transfer deterioration is limited. The smaller twist ratio results in better heat transfer and hence improved suppression of heat transfer deterioration. In an experimental investigation by Balaga et al. [26], the heat transport capability of hybrid nanofluid (f-MWCNT and Fe₂O₃) combined with twisted tape, perforated twisted tape and wire coil was studied. Due to significant improvement in flow dynamics, the wire coil and perforated twisted tape combination yielded the best result among the others. Alzahrani and Usman [27] conducted a numerical study on the plain tube subjected to natural circulation, having twisted tape (tight and loose fit, regularly spaced, and

variation in twist ratio). The results revealed that the heat transfer coefficient and pressure drop increase with the lower twist ratio. For full length twisted tapes, a 28% and 102.8% increase in heat transfer and pressure drop were observed, corresponding to 26% and 90% increment in case of regularly spaced twisted tape (inter-tape spacing equal to three times the diameter). For the case of different widths of the twisted tapes, both heat transfer coefficient and pressure drop increment was proportional to the tape width.

To date, literature review deliberated multiple heat transfer augmentation techniques in NCL [14], excluding binary fluids and turbulators. However, different combinations of binary fluids have been tried in heat pipes and pulsating heat pipes, which resulted in good heat transfer enhancement [15]–[17]. On the other hand, different turbulators have been extensively used in forced circulation systems [18]–[23]. Further, in a numerical study [27], the application of twisted tape in a vertical pipe (configured with natural circulation) was discussed, and better heat transfer augmentation was found at the cost of high-pressure drop.

Among different turbulators, the wire coil is most suitable for NCL due to notable heat transfer improvement at the least cost of pressure drop. On the other hand, with binary fluids, the natural circulation can be enhanced during heat addition due to different boiling points of two immiscible fluids. Owing to the passive mode of heat transfer augmentation in NCL, an experimental investigation is not yet explored.

Hence in the present study, the performance of NCL is experimentally investigated by considering binary fluid as well as wire coil. Since the pressure gain in the natural circulation system is due to the density difference of fluid, the pressure drop caused by the insert should be minimum. Hence selection of wire coil over twisted tape is justified. Concerning binary fluid, a greater density difference (higher flow rate) is expected due to fluid phase transition. However, due to the dissimilar boiling point of two fluids (in binary fluid), the NCL may experience instability during operation. Given this, instability analysis is also undertaken.

2. Theoretical background

The present HHHC loop has an L/d ratio (total length of the loop/loop diameter) of 300. Before taking up the experimental analysis, the loop behaviour is verified by referring to the widely used 1-D steady-state code by Vijayan et al. [7]. The loop material, size and aspect ratio (width/height) are different for the present loop compared to earlier studies. Hence, a thorough analysis is essential. Initially, with known values of loop dimensions, heat input (Q_{in}), condenser mass flow rate (\dot{m}_c) and coolant bulk temperature (T_c), cooler side and loop side convective heat transfer coefficients (h_i and h_o) are calculated as follows:

Cooler side Reynolds number is given as,

$$Re = \frac{\rho D_h V}{\mu} \quad (1)$$

The velocity of the coolant and cooler hydraulic diameter are,

$$V = \frac{\dot{m}}{\rho A} \quad (2)$$

$$D_h = \frac{\pi(D_i^2 - D_o^2)}{(\pi * D_o) + (\pi * D_i)} \quad (3)$$

Where the cross section area of the cooler is,

$$A = \frac{\pi}{4} (D_i^2 - D_o^2) \quad (4)$$

D_i is the inner diameter of the annulus and D_o is the outer diameter of the loop pipe.

Based on Re , an appropriate correlation is selected to determine Nu .

$$h_o = \frac{Nu_k}{D_h} \quad (5)$$

Assuming the bulk mean temperature of the loop T_b (K), the properties of the loop fluid are determined, which include density (ρ_o), specific heat (C_p), absolute viscosity (μ), thermal conductivity (k), thermal expansion coefficient (β_T).

The modified Grashof number Gr_m [11] is defined as,

$$Gr_m = \frac{D_r^3 \rho_o^2 \beta_T g Q_{in} H}{\mu^3 A C_p} \quad (6)$$

Where, A is cross sectional area of the loop, Q_{in} is heat input, and H is the centreline elevation

The geometric number N_G is determined as,

$$N_G = \frac{L_t}{D_r} \quad (7)$$

Where, L_t is total loop length and D_r is the inner diameter of the loop.

Steady state Reynolds number Re_{ss} [11] is calculated as,

$$Re_{ss} = \left[\frac{2 Gr_m}{p N_G} \right]^{\frac{1}{3-b}} = C \left(\frac{Gr_m}{N_G} \right)^r; r = \frac{1}{3-b}; C = \left[\frac{2}{p} \right]^{\frac{1}{3-b}} \quad (8)$$

Where, p and b are constants derived through friction factor testing and are as follows:

For laminar flow ($p = 3.89$; $b = 0.56$), transition flow ($p = 5.47$; $b = 0.62$) and turbulent flow ($p = 0.23$; $b = 0.22$).

Later, based on the Re_{ss} , Nu value is determined either using laminar or turbulent correlation as follows:

For laminar region and transition flow,

$$Nu = 4.365 \quad (9)$$

For turbulent flow Gnielinski correlation [28] is used, which is given as,

$$Nu_D = \frac{(f/8)(Re_D - 1000)Pr}{1 + 12.7(f/8)^{1/2}(Pr^{2/3} - 1)} \quad (10)$$

Further, Blasius correlation [29] is used to evaluate f

$$f = x Re^{-n}, \text{ where } x = 0.235 \text{ and } n = 0.22$$

Heat transfer co-efficient of the loop fluid is,

$$h_i = \frac{k * Nu_i}{D_i} \quad (11)$$

Where, D_i and k are loop inside diameter and thermal conductivity of loop fluid.

Overall heat transfer coefficient based on inside surface area is given as,

$$U_i = \frac{1}{\frac{1}{h_i} + \frac{L}{k} + \frac{1}{h_o}} \quad (12)$$

Where k and L are the thermal conductivity of stainless steel and the thickness of the loop.

Further, constant P is defined as,

$$P = \frac{4U_i A}{\dot{m}_l C_p} \quad (13)$$

Cold leg temperature,

$$T_{cl} = T_c + \frac{4Q_{in} A L h}{\dot{m}_l C_p} \left[\frac{1}{e^{PL_c} - 1} \right] \quad (14)$$

Where \dot{m}_l is mass flow rate of loop fluid.

Later using cold leg temperature, hot leg temperature is determined as,

$$T_{hl} = T_{cl} + \frac{4Q_{in} A L h}{\dot{m}_l C_p} \quad (15)$$

Once T_{cl} and T_{hl} are found, its mean temperature is termed as new bulk temperature given as $T_{b\ new}$. If the difference between $T_{b\ new}$ and assumed T_b is greater than 0.001, then the procedure is repeated as mentioned in the flowchart (Fig. 3).

Assumptions in the analysis are: no heat loss from the loop to the surrounding; the fluid flow rate is constant; no temperature gradient in the hot leg and cold leg; and temperature variation is one dimensional.

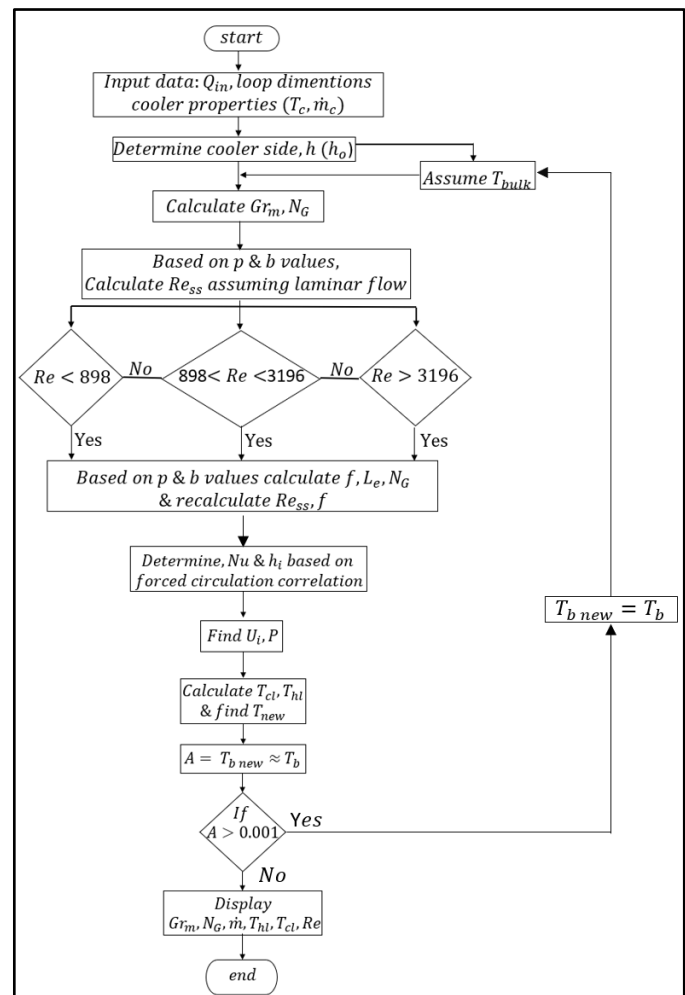


Fig. 3. Flowchart for analytical code

3. Experimental setup and operating procedure

This section briefs the calculation of friction factor, experimental setup, operating procedure, and subsequent data reduction process.

3.1. Determination of friction factor

The analytical code for NCL considers smooth pipe. However, commercially available tube possesses certain roughness. Hence the friction factor was evaluated experimentally for the SS pipe before fabricating the NCL.

The experiment was conducted for a mass flow rate of 0.2 kg/min to 4 kg/min (56 trials), which yields the *Re* in the range of 263 to 5500. Simultaneously the pressure drop across pipe length of 1.05 m was recorded to relate *Re* with pressure drop. Ultimately *f* vs *Re* characteristics is defined for laminar, transition and turbulent regimes by referring to Darcy-Weisbach [30].

3.2. Experimental setup

The schematic of the metal loop is shown in Fig. 4, and its geometrical details are enlisted in Table 1. The loop is constructed using a seamless SS 304 steel pipe. The four sections, viz., heater, hot leg, cold leg, and cooler, are joined to form an NCL. In the heater section, provisions are made to connect the differential pressure transmitter for pressure measurement. Initially, a mica sheet is wrapped around the heater region, which acts as an electrical insulator. Later, a nichrome wire (19 SWG) is closely wound over it to facilitate resistance heating. In the cooler region, an additional SS tube is welded over the loop pipe to form a double-pipe heat exchanger. Eight K-type thermocouples (mineral insulated with nut and ferrule arrangement, Ø 1.5 mm) are fixed along the hot and cold leg to measure the temperature of the loop fluid. Three more thermocouples S1, S2, and S3 (K-type, wire, Ø 0.4 mm), are attached to the surface of the heater to determine its surface temperature. Further, an expansion tank is connected from the bottom of the NCL, as shown. The entire loop is insulated using the ceramic blanket to avoid heat loss to the surrounding.

The wire terminals from the heater are connected to a dimmerstat through a power analyser (Yokogawa WT310E) to supply the known heat input to the loop. A differential pressure transmitter (Yokogawa EJX120A) is connected across the heater to measure the pressure drop, which is later used to determine the loop fluid mass flow rate. Further, a thermostatic bath (Siskin Profichill) and a mass flow meter (Rheonik RHM-08) are connected across the cooler to supply the coolant (water) at a constant temperature and flow rate. To measure the temperature difference across the cooler, two additional Pt-100 RTDs (stem type, Ø 5 mm) are fixed at the inlet and outlet of the cooler. Finally, all the thermocouples, power analyser, DPT, and mass flow meter terminals are connected to a data logger to capture real-time data.

The present study uses a wire coil as the turbulator (Fig. 5). It is prepared by a copper wire of Ø 0.5 mm with a pitch ratio (wire spacing/tube diameter) of 4. In case of binary fluid,

based on the total volume of the loop, water and acetone are mixed in the proportion of 60:40.

3.3. Experimental procedure

Experiments are conducted to observe the steady-state performance of the NCL with base fluid (water), binary fluid (water + acetone), and wire coil with base fluid by varying the heat input range from 100 W to 600 W.

- Initially, the loop is filled with water until the level reaches half of the expansion tank.
- With the pre-set value of coolant flow rate and temperature, flow is maintained in the cooler to stabilise the loop.
- A known wattage (heat flux) is supplied to the heater through the dimmerstat-power analyser arrangement.
- Data scanning is set to an interval of 5s to record all parameters.

Table 1. Loop dimensions

Parameters	Dimensions (mm)
Loop inner diameter, <i>d_i</i>	21.13
Loop outer diameter, <i>d_o</i>	25.50
Heater length, <i>L_h</i>	1000
Cooler length, <i>L_c</i>	1000
Cooler inner diameter, <i>D_i</i>	39.15
Cooler outer diameter, <i>D_o</i>	42.7
Vertical length, <i>L</i>	1800
<i>L_v/d</i>	298
Horizontal length, <i>H</i>	1200

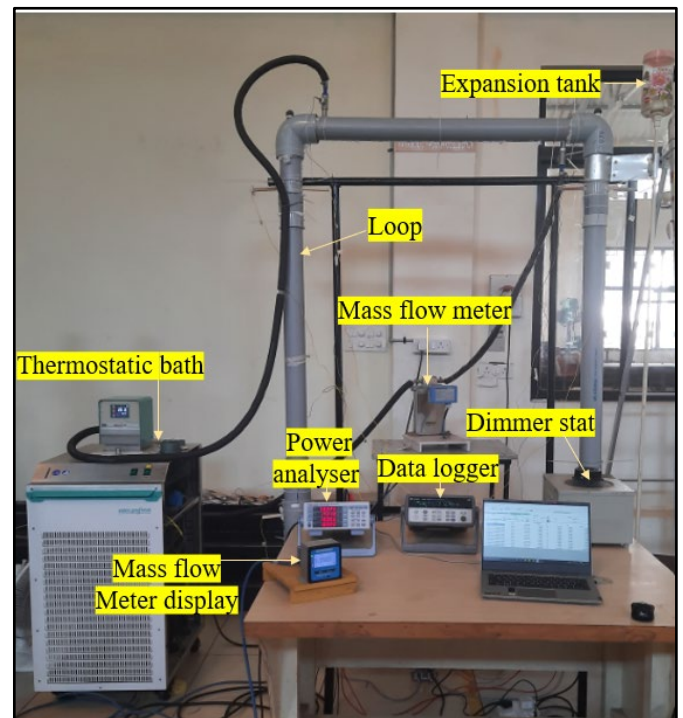


Fig. 4. Experimental test rig



Fig. 5. Wire coil

- The NCL runs continuously until a steady-state is attained (considering both differential pressure and ΔT across the cooler).
- The entire procedure is repeated for different heat inputs (100 – 600 W).
- Later the loop is completely filled with binary fluid.
- In case of turbulator experiments, a wire coil is inserted into the heater section, and the above said procedure is repeated.

3.4. Data reduction

Based on the friction factor testing, correlations are developed as follows and the subsequent parity plots are drawn (Fig. 6).

$$f = 3.892 * Re^{-0.562} \quad \text{for laminar region} \quad (16)$$

$$f = 5.474 * Re^{-0.620} \quad \text{for transition region} \quad (17)$$

$$f = 0.235 * Re^{-0.220} \quad \text{for turbulent region} \quad (18)$$

Mass flow rate is calculated using the pressure drop.

$$\dot{m} = \left(\frac{\Delta P * 2d_i}{\rho * L * \left(\frac{4}{\pi * \mu * d_i} \right)^n * \left(\frac{1}{\rho^2 * \left(\frac{\pi * d_i^2}{4} \right)^2} \right) * x} \right)^{\frac{1}{2+n}} \quad (19)$$

Where ρ, μ based on loop mean temperature, L be the length where line pressure is measured, d_i is the loop inside diameter and ΔP is the differential pressure. Finally, n and x values depend on the flow region (laminar, transient, and turbulent).

Heat gained in the cooler,

$$Q_c = m_c * C_p * \Delta T_c \quad (20)$$

Where ΔT_c is the difference in coolant entry and exit temperatures.

Thermal efficiency is defined as

$$\eta_{th} = \frac{Q_{out}}{Q_{in}} \quad (21)$$

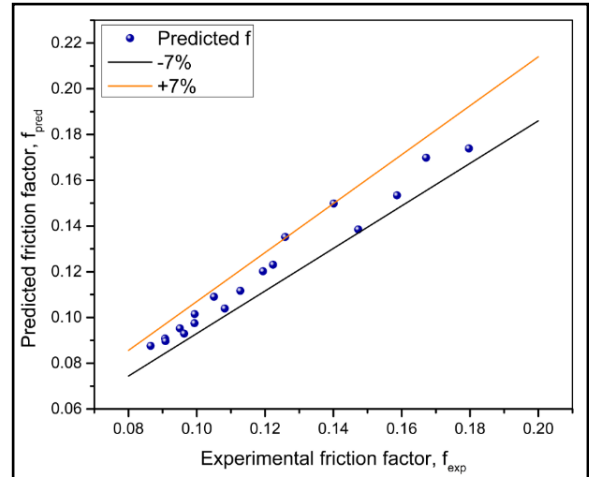
Where $Q_{out} = Q_c$

The heat input is taken from power analyser.

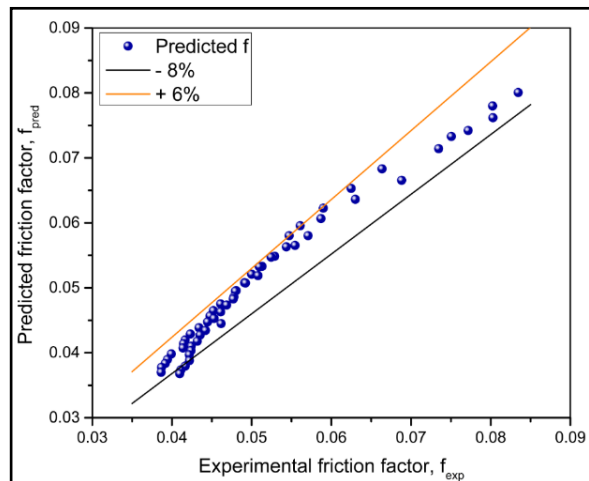
Heat transfer coefficient of loop fluid is,

$$Q = h A \Delta T \quad (22)$$

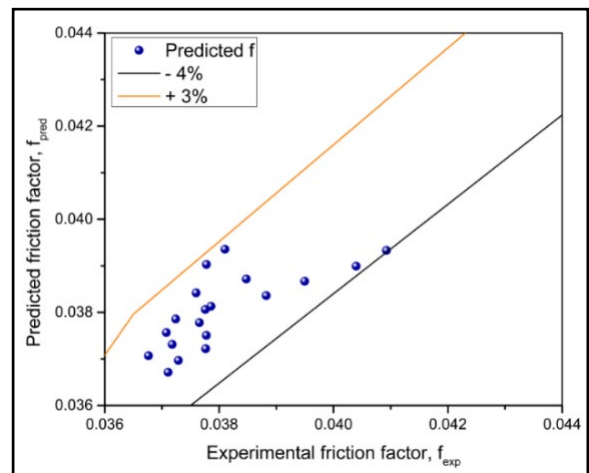
Where ΔT is the temperature difference between the heater surface and loop fluid and A is the heater surface area.



(a) Laminar region



(b) Transition region



(c) Turbulent region

Fig. 6. Parity plots for friction factor

4. Results and discussion

This section includes a comparison of present loop behaviour with the analytical code and the effect of turbulator and binary fluid on the loop stability and performance.

4.1. Loop validation

Initially, the NCL is analysed by incorporating Vijayan correlation [6]. Generally, steady state Re_{ss} of the loop is plotted against Gr_m / N_G ratio and compared with the standard analytical value. Most of the studies use modified Grashof number ratio and Reynolds number. Since both terms are dimensionless, it can be used for any loop irrespective of size. As shown in Fig. 7, the deviation observed is less than 5 %, and heat loss is the reason for it.

4.2. Effect of wire coil

Heat transfer augmentation and corresponding pressure drop due to the wire coil are discussed here.

4.2.1 Heat transfer augmentation

The loop with wire coil is tested at different wattages to check its stability and heat transfer augmentation. Interestingly the loop attains stability at a fixed time irrespective of the wattage, as shown in Fig. 8(a). Also, due to the presence of a wire coil in the heater, the fluid convective coefficient improves (Fig. 8(b)); thereby, the heater surface temperature drops, as depicted in Fig. 8(c). Ultimately it leads to efficiency improvement, as shown in Fig. 8(d). The boundary layer rupture is the main cause for this improvement. As inserts are very effective at low Re , it is worth noting that at heat inputs of 200 W and 300 W, the wire coil effect is significant as the fluid flow regime lies between laminar and transition.

4.2.2 Pressure drop

The heat transfer enhancement by wire coil is at the cost of additional pressure drop. Generally, the mass flow rate of loop fluid is measured indirectly through the pressure drop or temperature drop method. Due to higher heat input or some other means, the flow rate increases, and the corresponding pressure drop also increases. Accordingly, the temperature difference across the heater reduces. However, in the present case, the rise in pressure drop is solely due to the insertion of a wire coil, which is of the order of 3.5-4.5 times compared to a conventional loop (Fig. 9(a)). Further, to confirm the drop in flow rate, the loop fluid temperature difference across the heater was plotted as shown in Fig. 9(b), which depicted a 1.2-1.3 times higher value than the without wire coil case. Thus, it can be deduced that in the case of NCL with turbulator, the differential pressure must not be used for loop fluid flow rate calculation, and only the temperature difference across the heater serves the purpose. The wire coil in the present loop enhanced the heat transfer coefficient by 0.2-5.5% at the cost 26-30% decrease in loop mass flow rate. However, it tends to be the best as other inserts lead to still higher pressure drop.

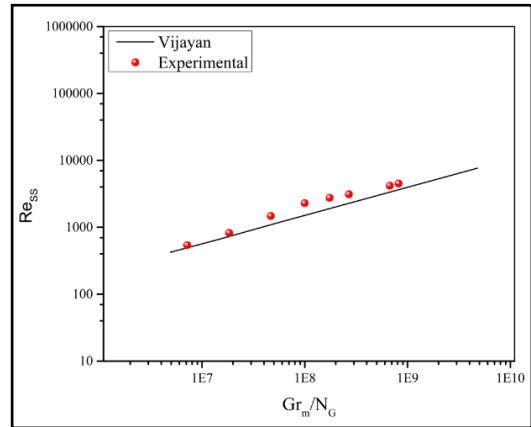
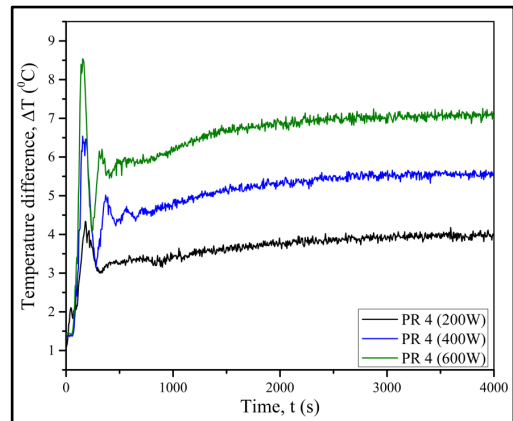
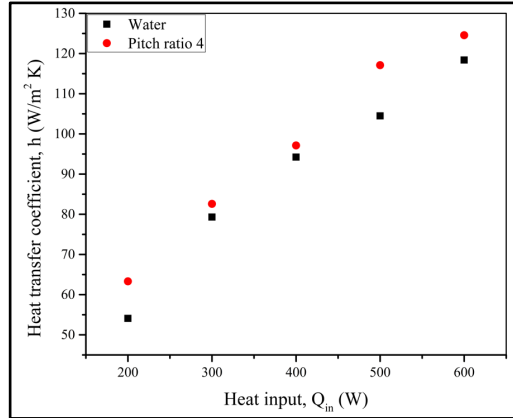


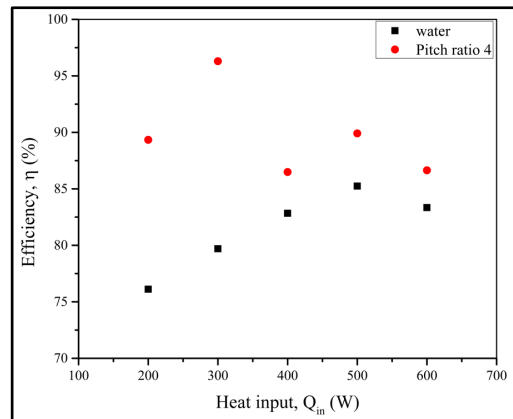
Fig. 7. Loop validation with Vijayan code [7]



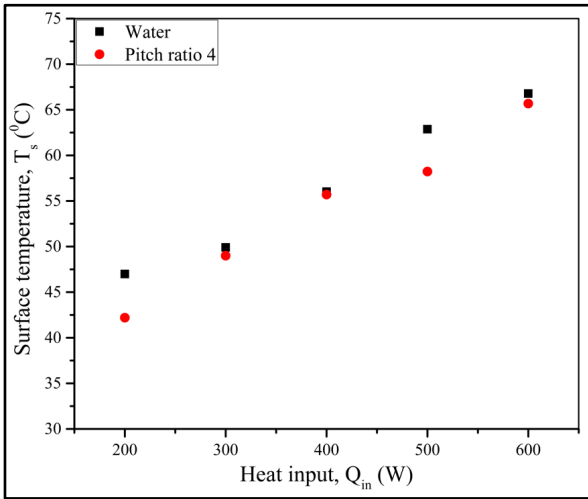
(a) Loop stability



(b) Heat transfer coefficient

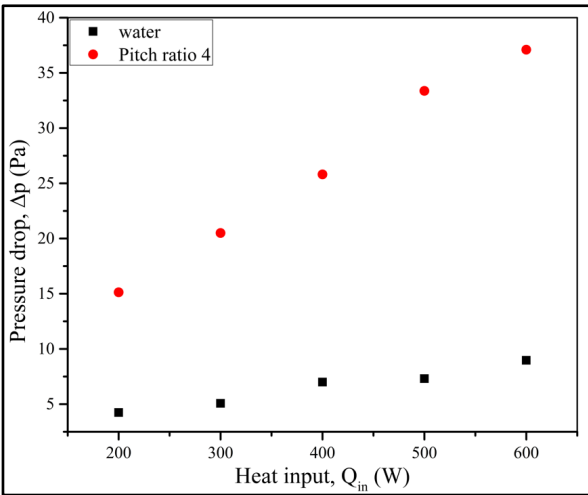


(c) Efficiency

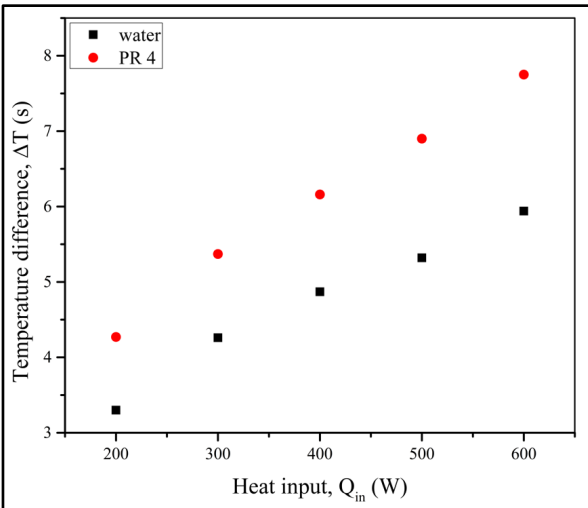


(d) Surface temperature

Fig. 8. Heat transfer augmentation due to wire coil



(a) Pressure drop



(b) Temperature difference

Fig. 9. Pressure characteristics for wire coil

4.3. Effect of binary fluids

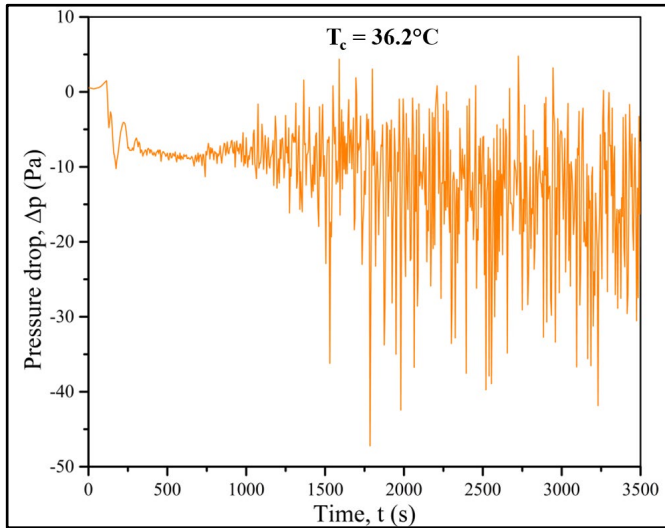
The influence of coolant temperature and flow rate on the stability of binary fluid based NCL is discussed here.

4.3.1 Influence of coolant temperature

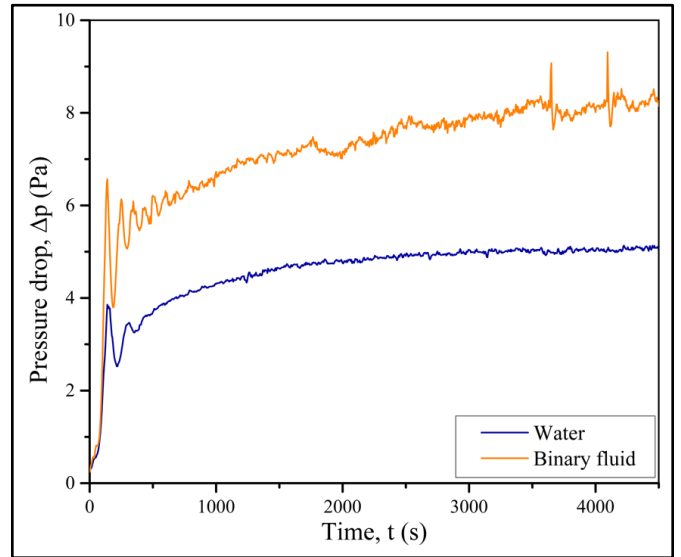
In the binary fluid (40 % acetone + 60 % water), acetone begins to boil at $\approx 56^\circ\text{C}$. Hence, if the heater surface is maintained close to the boiling point of acetone, a higher driving force is expected because of the greater density difference. If the surface temperature exceeds, the loop becomes highly unstable due to change in the fluid phase. However, in the present setup, since the heater surface temperature difficult to control, only the coolant entry temperature is varied.

Initially, the NCL is subjected to 600 W and a coolant entry temperature of 36.2°C . As depicted in Fig. 10(a), the loop becomes highly unstable, indicating the acetone phase conversion in the heater region and not being effectively cooled by the other immiscible liquid. Hence, in the next trial, the coolant temperature for the same heat input is reduced to 13.7°C , and the loop becomes stable right from the beginning, as shown in Fig. 10(b). Later, to check the upper threshold of the coolant temperature, 15.8°C was maintained, and within 100 s, the loop became unstable. Hence for the heat load of 600 W, the appropriate coolant temperature should be less than 15.8°C . Later, a heat load of 400 W with a coolant temperature of 36.3°C is undertaken to confirm this behaviour. Although the loop is stable during the initial 1500 s, bi-directional oscillations commenced later and amplified to a greater extent, as shown in Fig. 10(c). Hence the coolant temperature was reduced to 25°C , which showed improvement in stability. Hence it was further reduced, and at 22°C , the loop became stable. Therefore in the case of binary fluid, the role of coolant temperature is crucial.

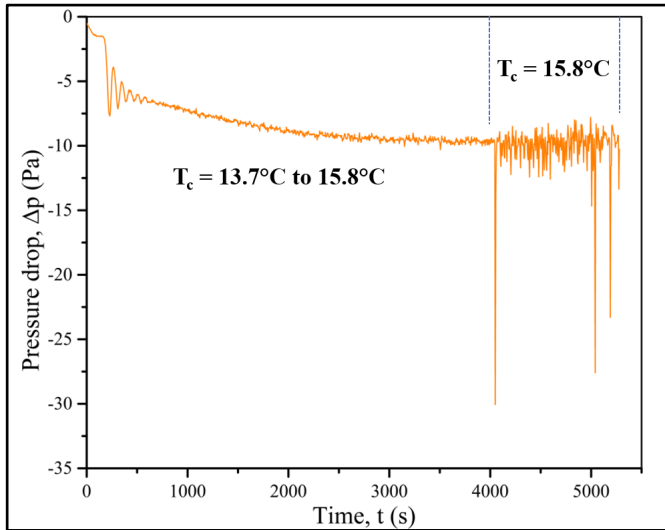
Having noted the coolant temperature influence, in the next stage, the coolant temperature is set to 24.5°C , and the performance of the loop with different heat inputs is tested and compared with base fluid, i.e., water. For 300 W, with binary fluid, although the loop is stable, periodic oscillations are seen (Fig. 11(a)), which indicates the stability threshold for this setting. The test is continued at 400 W (maintaining the coolant entry temperature constant at 24.5°C), and unidirectional pulsing is seen (Fig. 11(b)). Later, in case of 600 W, the loop became highly unstable with an amplitude value as high as the base value, as depicted in Fig. 11(c). For the fixed coolant entry temperature, the loop was nearly stable at 300 W, unidirectional pulsing was lower at 400 W, and became completely unstable at 600 W. However, under the same operating condition, NCL with water showed stability. This is due to a higher boiling point compared to acetone. It is worth noting that the pressure difference noticed with binary fluid is more than the water.



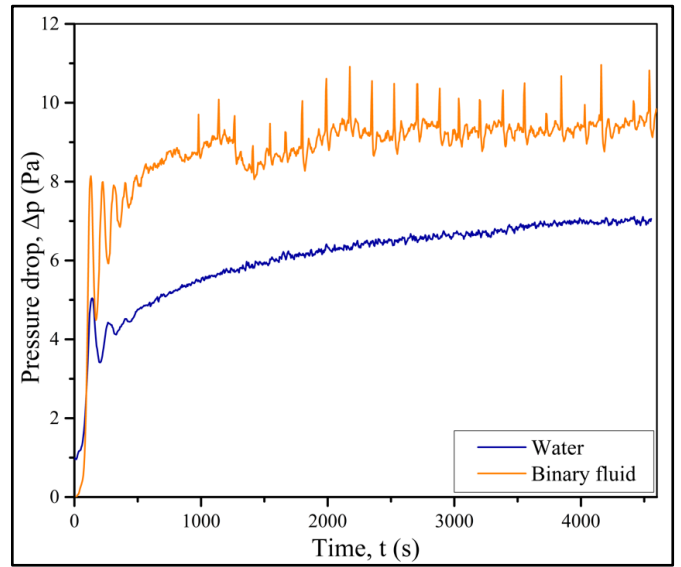
(a) 600W with constant T_c



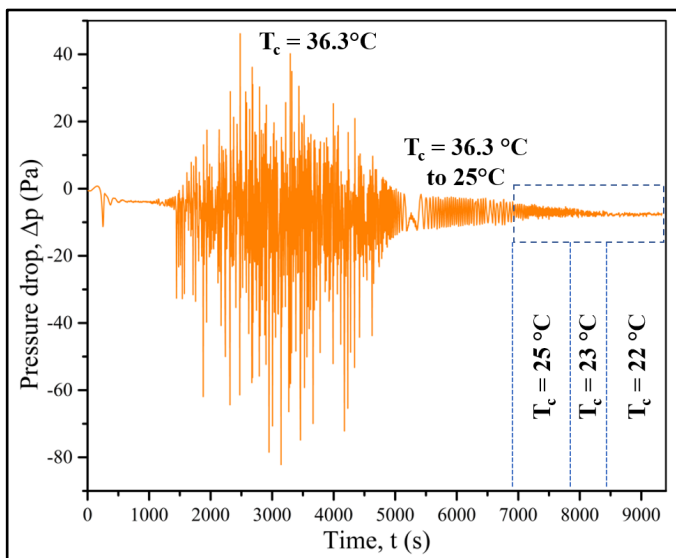
(a) 300 W Heat input



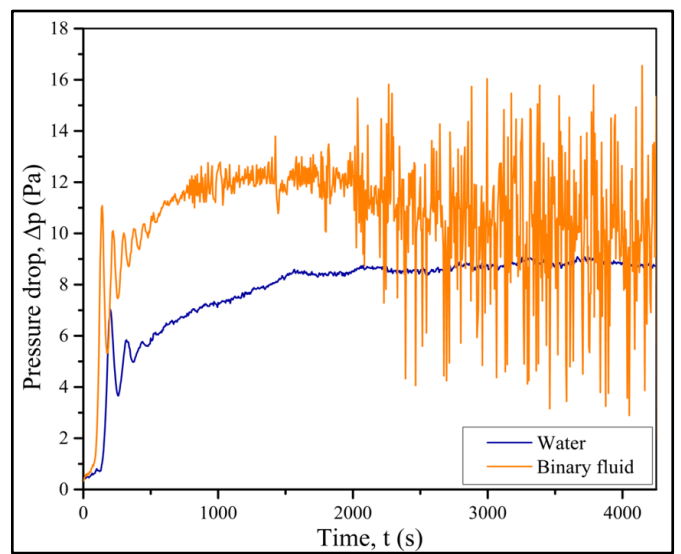
(b) 600W with varying T_c



(b) 400 W Heat input



(c) 400W with varying T_c



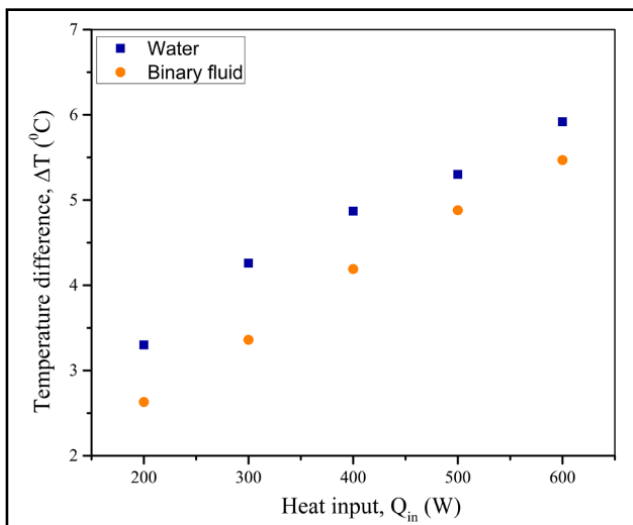
(c) 600 W Heat input

Fig. 10. Effect of coolant temperature on loop stability

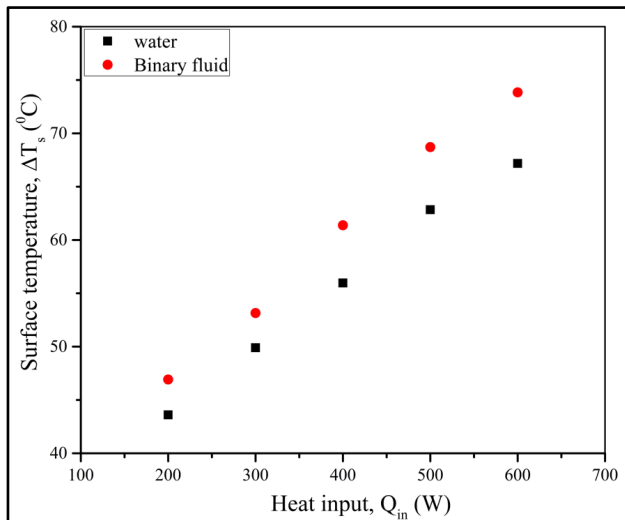
Fig. 11. Effect of binary fluid on loop pressure drop

4.3.2 Heat transfer characteristics

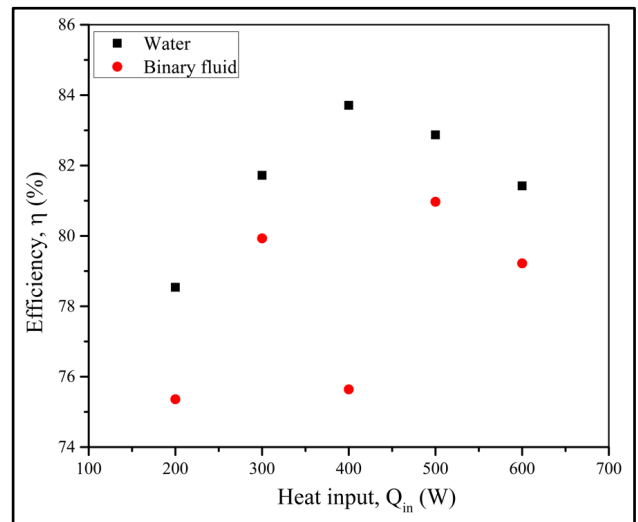
As seen in Fig. 11, for every wattage, the pressure difference is more for binary fluid than water. This trend is beneficial as a higher pressure difference is an indication of a higher flow rate of fluid within the loop. Hence to confirm this behaviour, the temperature difference across the heater is plotted, which shows a negative trend (Fig. 12(a)). Further, both surface temperature (Fig. 12(b)), as well as loop efficiency (Fig. 12(c)) are also in favour of a lower flow rate compared to water. This is because the heat carrying capacity of acetone ($C_p = 2160 \text{ J/kgK}$) is half of that of water. Therefore even with the increase in mass flow rate, the amount of heat carried by the binary fluid is less, resulting in an increase in the surface temperature of the heater section.



(a) Temperature difference



(b) Surface temperature



(c) Efficiency

Fig. 12. Characteristics of binary fluid-based loop

5. Conclusion and future scope

The present experimental investigation revealed the effect of wire coil (pitch ratio =4) and binary fluid (water:acetone (60:40)) in NCL as detailed below:

- i. The preliminary testing of the loop yielded different correlations for the loop friction factor with an accuracy level of -8 to +7%. The loop performance is then validated against the analytical code, which found very good agreement.
- ii. Since the L/d ratio of the loop is ≈ 300 , the loop is found to be stable for the range of heat input.
- iii. The use of wire coil as a turbulator led to a 4.86-11.45% increase in the convective heat transfer coefficient. However, the increase in temperature difference across the legs suggests that the heat transfer enhancement is at the cost of decrement in the loop flow rate.
- iv. Incorporating acetone as binary fluid led to an augmentation in loop flow rate, confirmed by a 10.75% increment in differential pressure and a 4.86% decrement in temperature difference across legs. However, due to the low specific heat of acetone, this flow rate enhancement is not reflected in terms of efficiency improvement or surface temperature reduction.

The obtained results also defined the scope for future work as listed below:

- i. Heat transfer augmentation can be further effective if discretised wire coil is adopted.
- ii. With base fluid, heavier fluid can be injected at one end and taken out at the other end to enhance the driving force.
- iii. With a combination of binary fluid and discretised turbulator in the loop, more heat can be extracted from the heater side with a higher mass flow rate.

References

- [1] A. G. Alkholidi and H. HAMAM, "Solar Energy Potentials in Southeastern European Countries: A Case Study," *Int. J. Smart grid*, 2019, doi: 10.20508/ijsmartgrid.v3i2.51.g55.
- [2] A. Harrouz, A. Temmam, and M. Abbes, "Renewable Energy in Algeria and Energy Management Systems," *Int. J. Smart grid*, 2017, doi: 10.20508/ijsmartgrid.v2i1.10.g9.
- [3] M. Banja and M. Jégard, "An Analysis of Capacity Market Mechanism for Solar Photovoltaics in France," *Int. J. Smart grid*, 2019, doi: 10.20508/ijsmartgrid.v3i1.36.g41.
- [4] D. Siswanto and S. L. Z. Ridho, "Is Grid Solar Power Still Attractive Amid Decreasing Fuel Prices? The Case of Indonesian Electrical Power," *Int. J. Smart grid*, Jun. 2021, doi: 10.20508/ijsmartgrid.v5i2.188.g148.
- [5] F. Javed, "Impact of Temperature & Illumination for Improvement in Photovoltaic System Efficiency," *Int. J. Smart grid*, no. v6i1, 2022, doi: 10.20508/ijsmartgrid.v6i1.222.g185.
- [6] P. K. Vijayan, A. K. Nayak, D. Saha, and M. R. Gartia, "Effect of Loop Diameter on the Steady State and Stability Behaviour of Single-Phase and Two-Phase Natural Circulation Loops," *Sci. Technol. Nucl. Install.*, vol. 2008, pp. 1–17, 2008, doi: 10.1155/2008/672704.
- [7] P. K. Vijayan, M. Sharma, and D. Saha, "Steady state and stability characteristics of single-phase natural circulation in a rectangular loop with different heater and cooler orientations," *Exp. Therm. Fluid Sci.*, vol. 31, no. 8, pp. 925–945, Aug. 2007, doi: 10.1016/j.expthermflusci.2006.10.003.
- [8] K. Naveen, K. N. Iyer, J. B. Doshi, and P. K. Vijayan, "Investigations on single-phase natural circulation loop dynamics. Part 3: Role of expansion tank," *Prog. Nucl. Energy*, vol. 78, pp. 65–79, Jan. 2015, doi: 10.1016/j.pnucene.2014.08.007.
- [9] R. Saha, S. Sen, S. Mookherjee, K. Ghosh, A. Mukhopadhyay, and D. Sanyal, "Experimental and Numerical Investigation of a Single-Phase Square Natural Circulation Loop," *J. Heat Transfer*, vol. 137, no. 12, Dec. 2015, doi: 10.1115/1.4030926.
- [10] S. Nakul and U. C. Arunachala, "Stability and thermal analysis of a single-phase natural circulation looped parabolic trough receiver," *Sustain. Energy Technol. Assessments*, vol. 52, p. 102242, Aug. 2022, doi: 10.1016/j.seta.2022.102242.
- [11] P. K. Vijayan, A. K. Nayak, and N. Kumar, *Single-Phase, Two-Phase and Supercritical Natural Circulation Systems*, 1st ed. Woodhead Publishing - Elsevier, 2019.
- [12] Y. Wang, X. Wang, H. Chen, H. Fan, R. A. Taylor, and Y. Zhu, "CFD Simulation of an Intermediate Temperature, Two-phase Loop Thermosiphon for Use as a Linear Focus Solar Receiver," *Energy Procedia*, vol. 105, pp. 230–236, May 2017, doi: 10.1016/j.egypro.2017.03.307.
- [13] D. N. Elton, U. C. Arunachala, and P. K. Vijayan, "Stabilization of single phase rectangular natural circulation loop of larger diameter using orifice plate," *Int. Commun. Heat Mass Transf.*, vol. 137, p. 106216, Oct. 2022, doi: 10.1016/j.icheatmasstransfer.2022.106216.
- [14] D. N. Elton and U. C. Arunachala, "Status, Trends and Significance of Single Phase, Single and Coupled Natural Circulation Loops in Sustainable Energy Technologies – A comprehensive review," *Int. J. Renew. Energy Res.*, no. v11i3, Sep. 2021, doi: 10.20508/ijrer.v11i3.12330.g8239.
- [15] P. R. Pachghare and A. M. Mahalle, "Effect of Pure and Binary Fluids on Closed Loop Pulsating Heat Pipe Thermal Performance," *Procedia Eng.*, vol. 51, pp. 624–629, 2013, doi: 10.1016/j.proeng.2013.01.088.
- [16] P. R. Pachghare and A. M. Mahalle, "Thermo-hydrodynamics of closed loop pulsating heat pipe: an experimental study," *J. Mech. Sci. Technol.*, vol. 28, no. 8, pp. 3387–3394, Aug. 2014, doi: 10.1007/s12206-014-0751-9.
- [17] X. Cui, Z. Qiu, J. Weng, and Z. Li, "Heat transfer performance of closed loop pulsating heat pipes with methanol-based binary mixtures," *Exp. Therm. Fluid Sci.*, vol. 76, pp. 253–263, Sep. 2016, doi: 10.1016/j.expthermflusci.2016.04.005.
- [18] B. Kumar, G. P. Srivastava, M. Kumar, and A. K. Patil, "A review of heat transfer and fluid flow mechanism in heat exchanger tube with inserts," *Chem. Eng. Process. - Process Intensif.*, vol. 123, pp. 126–137, Jan. 2018, doi: 10.1016/j.cep.2017.11.007.
- [19] M. Awais and A. A. Bhuiyan, "Heat transfer enhancement using different types of vortex generators (VGs): A review on experimental and numerical activities," *Therm. Sci. Eng. Prog.*, vol. 5, pp. 524–545, Mar. 2018, doi: 10.1016/j.tsep.2018.02.007.
- [20] C. Maradiya, J. Vadher, and R. Agarwal, "The heat transfer enhancement techniques and their Thermal Performance Factor," *Beni-Suef Univ. J. Basic Appl. Sci.*, vol. 7, no. 1, pp. 1–21, Mar. 2018, doi: 10.1016/j.bjbas.2017.10.001.
- [21] S. Liu and M. Sakr, "A comprehensive review on passive heat transfer enhancements in pipe exchangers," *Renew. Sustain. Energy Rev.*, vol. 19, pp. 64–81, Mar. 2013, doi: 10.1016/j.rser.2012.11.021.
- [22] M. Sheikholeslami, M. Gorji-Bandpy, and D. D. Ganji, "Review of heat transfer enhancement methods: Focus on passive methods using swirl flow devices," *Renew. Sustain. Energy Rev.*, vol. 49, pp. 444–469, Sep. 2015, doi: 10.1016/j.rser.2015.04.113.
- [23] M. H. Mousa, N. Miljkovic, and K. Nawaz, "Review of heat transfer enhancement techniques for single phase flows," *Renew. Sustain. Energy Rev.*, vol. 137, p. 110566, Mar. 2021, doi: 10.1016/j.rser.2020.110566.
- [24] O. Keklikcioglu and V. Ozceyhan, "Heat transfer augmentation in a tube with conical wire coils using a

- mixture of ethylene glycol/water as a fluid,” *Int. J. Therm. Sci.*, vol. 171, p. 107204, Jan. 2022, doi: 10.1016/j.ijthermalsci.2021.107204.
- [25] T. Cong, B. Wang, and H. Gu, “Numerical analysis on heat transfer enhancement of sCO₂ in the tube with twisted tape,” *Nucl. Eng. Des.*, vol. 397, p. 111940, Oct. 2022, doi: 10.1016/j.nucengdes.2022.111940.
- [26] R. Balaga, R. Koon, and S. Tunuguntla, “Heat transfer enhancement of the f-MWCNT- Fe₂O₃/Water hybrid nanofluid with the combined effect of wire coil with twisted tape and perforated twisted tape,” *Int. J. Therm. Sci.*, vol. 184, p. 108023, Feb. 2023, doi: 10.1016/j.ijthermalsci.2022.108023.
- [27] S. Alzahrani and S. Usman, “CFD simulations of the effect of in-tube twisted tape design on heat transfer and pressure drop in natural circulation,” *Therm. Sci. Eng. Prog.*, vol. 11, pp. 325–333, Jun. 2019, doi: 10.1016/j.tsep.2019.03.017.
- [28] A. Satou, H. Madarame, and K. Okamoto, “Unstable behavior of single-phase natural circulation under closed loop with connecting tube,” *Exp. Therm. Fluid Sci.*, vol. 25, no. 6, pp. 429–435, Dec. 2001, doi: 10.1016/S0894-1777(01)00092-9.
- [29] T. L. Bergman, F. P. Incropera, D. P. DeWitt, and A. S. Lavine, *Fundamentals of heat and mass transfer*, 8th ed. John Wiley & Sons, Inc., 2018.
- [30] C. F. COLEBROOK, “Turbulent flow in pipes, with particular reference to the transition region between the smooth and rough pipe laws,” *J. Inst. Civ. Eng.*, vol. 11, no. 4, pp. 133–156, Feb. 1939, doi: 10.1680/ijoti.1939.13150.